Sports Eng (2011) 14:139–146
DOI 10.1007/s12283-011-0074-3

ORIGINAL ARTICLE

Football boundary-layer separation via dust experiments

J. E. Goff · W. H. Smith · M. J. Carré

Published online: 30 October 2011

Abstract A method of examining the separation of the boundary layer of air from a sports ball, specifically a football, is presented. Using a ball launcher, a non-spinning football is fired into a dust cloud. A high-speed camera records the ball passing through the dust cloud. Unlike wind-tunnel methods, the dust method described here allows for the examination of the boundary-layer separation without a ball-supporting arrangement. Boundary-layer separation for speeds surrounding the drag crisis is studied. Though the general trend is for the boundary layer to separate farther back on the ball as the ball's centre-of-mass speed increases, anomalous behaviour is seen just past the drag crisis, namely a rise in the separation angle, followed by an expected decrease.

Keywords Football · Soccer · Aerodynamics · Transition · Drag · Boundary layer · Separation

Abbreviations

A	Projected area of sphere
a	Fitting parameter for drag data
b	Fitting parameter for drag data
C_D	Drag coefficient
D	Football diameter
F_D	Drag force
g	Acceleration due to gravity
m	Football mass
Re	Reynolds number
v	Football centre-of-mass velocity of the air
v_c	Fitting parameter for drag data
v_s	Fitting parameter for drag data
ν	Kinematic viscosity
ρ	Density of the air
φ	Boundary-layer separation angle
ω	Football angular speed

J. E. Goff (✉) · W. H. Smith
Department of Physics, Lynchburg College, Lynchburg, VA 24501, USA
e-mail: goff@lynchburg.edu

M. J. Carré
Department of Mechanical Engineering, University of Sheffield, Mappin Street, Sheffield S1 3JD, UK

1 Introduction

Fascination with the behaviour of footballs in flight has stimulated much research over recent years, delivered in a variety of ways. The most common way of measuring accurate aerodynamic coefficients is widely regarded to be through wind-tunnel testing. This began with ground-breaking work from Achenbach examining the aerodynamics of rough spheres [1] and has since been applied to footballs both using models of balls [2] and comparing actual designs of ball [3–5]. Although it is clear that these studies provide crucial understanding, wind tunnel testing tends to be somewhat limited by the fact that the ball has to be held firmly in place, usually by a rear-mounted support, which will undoubtedly affect the aerodynamics. CFD studies have also been carried out on sports balls [6], but these require simplifications and assumptions to be made, which limit the usefulness of the findings for real-world applications.

Recent advances in technology and improvements in affordability have led to the increased adoption of video analysis of trajectories to calculate aerodynamic coefficients of footballs. These include measurements made from simulated kicks, using a projection machine [7–9] as well

as from real kicks [10, 11]. In the latter study, flow visualisation was also achieved through the novel method of painting the balls with titanium tetrachloride before they were kicked, although the toxic nature of this substance meant that the human subjects had to wear protective suits and face masks [11].

This study is concerned with the development of a lab-based technique to carry out flow visualisation on actual footballs in flight, without the need for wind tunnels, and the study's explicit purpose is to determine the angle at which the boundary layer separates. It is hoped that results from such a technique will complement those from other studies and add to the overall understanding of football aerodynamics.

2 Football aerodynamics

During its flight through air, a football experiences a force from the air and the Earth's gravitational pull. This study used a 32-panel football manufactured by Umbro, model X III 250. With the ball's mass $m = 0.424$ kg, the gravitational pull on the ball from the Earth, i.e. the ball's weight, is $mg = 4.155$ N, where $g = 9.80$ m/s^2, the magnitude of gravitational acceleration. With a constant gravitational force on the ball, the more interesting force on the ball is the one from the air.

The air exerts a single force on the ball, though convention dictates that force is separated into three components because of the ball moving through, in general, three spatial dimensions. Figure 1 shows a free-body diagram of a football moving through air. One component of the air force is called "drag," and it points opposite the ball's velocity. The magnitude of the drag force [12] is $F_D = \frac{1}{2} \rho A C_D v^2$, where ρ is the air density (1.2 kg/m^3), A is the cross-sectional area of the football (0.0375 m^2), C_D is the dimensionless drag coefficient, and v is the ball's centre-of-mass speed with respect to the still air far from the ball. The drag coefficient depends on the ball's speed and its rate of spin. See Fig. 2 for a plot of the drag coefficient versus ball speed for a non-spinning 32-panel Fevernova ball as measured in a wind tunnel [3]. Figure 2 shows a curve fitted to the experimental data. The precipitous drop in the drag coefficient around 12.5 m/s is called the drag crisis [12].

Some researchers prefer to use Reynolds numbers instead of ball speed. The dimensionless Reynolds number is defined as $Re = vD/\nu$, where D is the ball's diameter (0.2184 m) and ν is the kinematic viscosity (1.54×10^{-5} m^2/s). A simple conversion between Reynolds number and speed for a football is $Re \times 10^{-5} \approx v/(7\text{ m/s}) \approx v/(16\text{ mph})$. Football is played mostly in the speed range 10 mph $< v <$ 70 mph, meaning $63{,}000 < Re < 440{,}000$ is roughly the range of Reynolds numbers for the game of football.

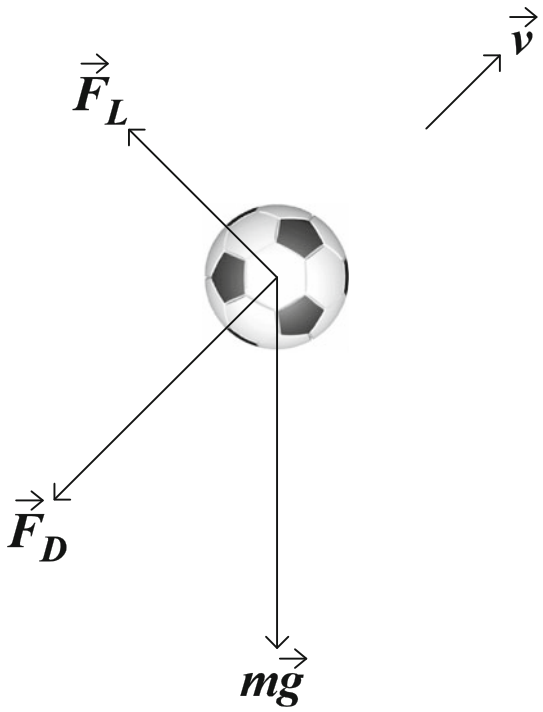

Fig. 1 Free-body diagram for a football moving through air. The figure shows a ball kicked with backspin, leading to a lift force with a component pointing up. If the ball's rotation axis were not pointing perpendicular to the page, a sideways component of the Magnus force would point perpendicular to the page

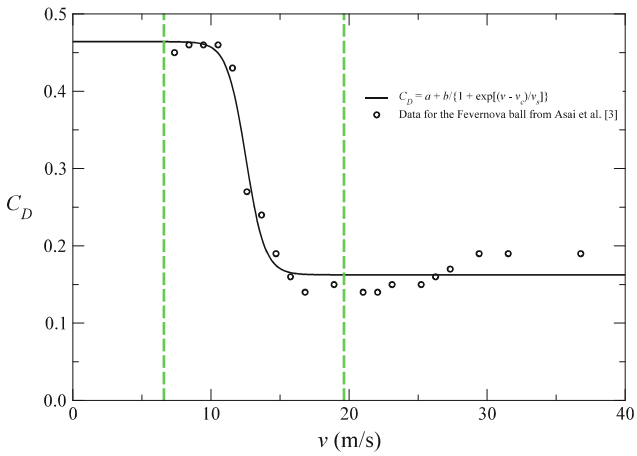

Fig. 2 Wind-tunnel data for a 32-panel Fevernova football from Asai et al. [3]. The *solid curve* is a fit to the data with $a = 0.16271$, $b = 0.30155$, $v_c = 12.5302$ m/s, and $v_s = 0.684205$ m/s. The *vertical dashed lines* demarcate the range of speeds used in this study's dust experiments

If the ball is spinning, the two components of the air force perpendicular to the drag force are the components of the Magnus force. The component in the direction of $\vec{\omega} \times \vec{v}$ is called "lift," where $\vec{\omega}$ is the angular velocity of the

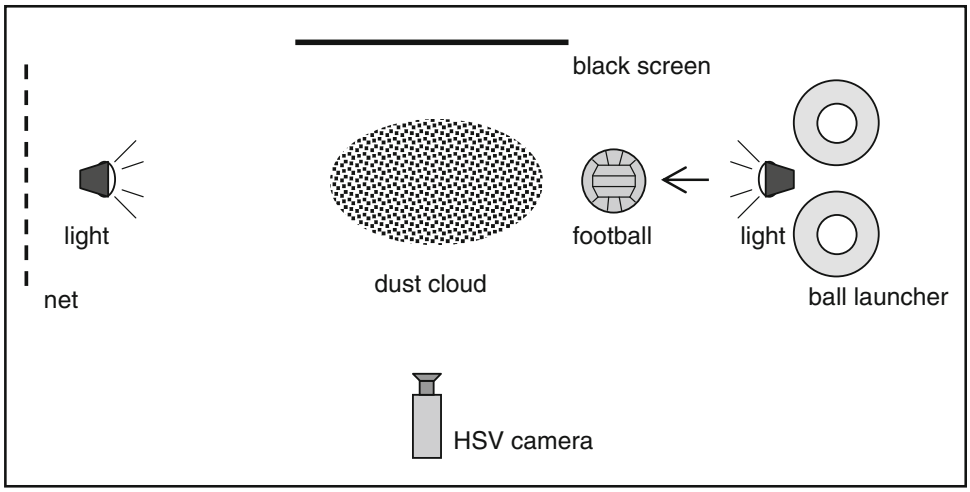

Fig. 3 Schematic diagram of the filming set-up (view from above). A football is shown immediately after being fired using the ball launcher. The black screen provides a dark background for filming and the net on the left catches the ball after it has left the filming region. The light is placed on the ground, below the path of the ball and is protected from any collision after the net has caught the ball. The person who claps the dust (not shown) stands adjacent to the black screen on the net side

spinning ball and $\vec{v}$ is the ball's centre-of-mass velocity with respect to the ground. The component perpendicular to both the drag and lift components is the "sideways" component. That force component is responsible for many of the spectacular curved kicks. Because the work here concentrates solely on balls without spin, force components associated with spin will not be discussed any further.

3 Experimental technique

Figure 3 shows a schematic aerial view of the test set-up. The launcher consists of four counter-rotating wheels that allow for the variation of the ball's centre-of-mass speed and spin rate. Because only balls with no spin are considered, the two wheels on the left side of the launcher are set to spin at the same rate as the two wheels on the right side of the launcher, but in the opposite direction. After leaving the launcher, the football travels about 2 m before entering a dust cloud. The dust cloud is created just before the ball is dropped into the launcher. An experimenter stands adjacent to the black screen seen in Fig. 3, on the far side from the launcher. A handful of standard, commercially available rock-climbing chalk dust (a powdered form of magnesium carbonate) is clapped from a height of about 2 m above the centre of the white rectangular cardboard that sits in front of the black cloth. To "clap" the dust means simply to hold a few grams of dust in one's hand, vigorously clap one's hands once or twice, and allow the dust to fall in a region where the football will pass. A few tries will be needed to ascertain the right amount of dust needed and the timing of the clap. Once the dust is clapped into the region of interest, the football is fired from the launcher and travels through the dust cloud. Located about 2.5 m from the centre of the dust cloud, the high-speed camera records the football's flight at the rate of 2,000 frames per second with a 512 × 256 pixel resolution. The camera's software creates a movie file in a "cine" format. CINE VIEWER[1] then converts the cine to AVI format. In-house software[2] is then used to analyse the frame-by-frame motion of the ball.

Figure 4 shows what is recorded and analysed in a typical launch. Each circle denotes the position of the football in 2.5-ms increments, i.e. every five frames recorded by the high-speed camera. Though the capability of analysing the ball's motion using all recorded frames exists, little accuracy is gained in going from analysing the ball's motion in 2.5-ms increments to analysing it in 0.5-ms increments. There are 11 frames shown in Fig. 4, all of which comprise 25 ms of the ball's flight time. Using the football's diameter as a standard of reference, the centre of the circle in the 1st frame is 47.6 cm from the centre of the circle in the 11th frame, thus establishing that the camera records about half a metre of horizontal flight distance for each launch. The average speed of the football shown in Fig. 4 is approximately 0.476 m/0.025 s ≈ 19.0 m/s. A more accurate determination of the average speed using the two-dimensional Cartesian coordinates of the ball's centre of mass from the 11 frames and numerical differentiation gives 19.14 m/s. The ball's speed for the launch shown in Fig. 4 drops only a little more than 3% during the 25 ms of motion that was analysed. Because balls launched at smaller speeds have smaller drag, it is found that for all trials, the football's centre-of-mass speed drops by no more than 4% as it passes through the camera's viewing region.

Once an average speed for a given trial is established, the angle φ at which the boundary layer separates from the football is determined. Figure 5 shows a schematic of how the angle φ is defined. The separation angle is found by

[1] This is produced by Phantom and may be downloaded for free at www.visionresearch.com/index.cfm?page=software.

[2] Originally developed by Richard Dignall and Simon Goodwill at the University of Sheffield.

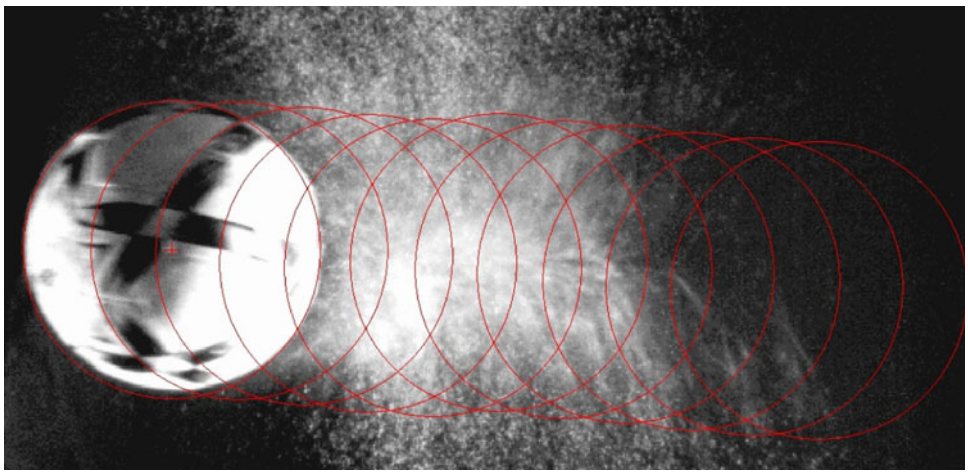

Fig. 4 A football moves at an average speed of approximately 19 m/s through a dust cloud. The distance between the centre-of-mass points for the *first circle* and the *last circle* is 47.6 cm. *Adjacent circles* are separated in time by 0.0025 s

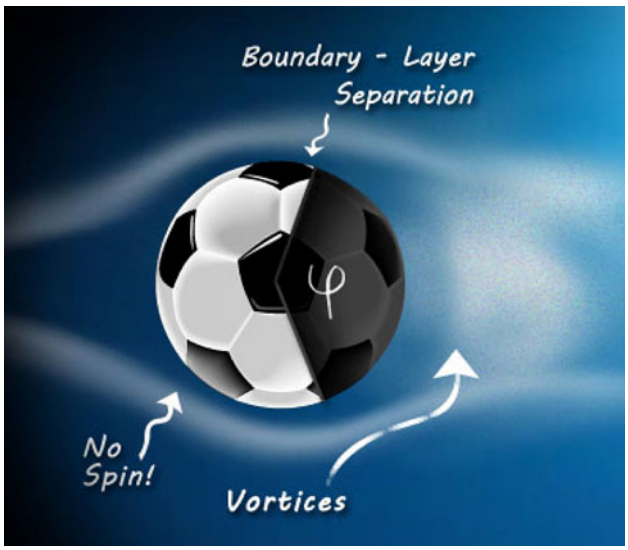

Fig. 5 Schematic of how the boundary-layer separation angle φ is defined. Image by Tracy Chase

examining the football as it passes through the dust cloud. A clear separation of the dust off the top and bottom of the ball is identified. Care must be taken to ensure that shadows created by the illuminating sources are not mistaken for points of boundary-layer separation. It helps to step frame by frame through each movie, both forwards and backwards, to be certain about the location of boundary-layer separation. Because just one camera films the football's motion, the boundary-layer separation angle is found in a single plane. No claims are made here about the location of boundary-layer separation on the other parts of the three-dimensional football.

Figure 6 shows two still images of footballs passing through dust clouds. The left image is that of a ball moving at a speed below the drag crisis, whereas the right image is that of a ball moving at a speed past the drag crisis. Note that a few initial trials had to be discarded as the art of creating a dust cloud in just the right place and launching the ball at just the right time were developed. An advantage of this dust-cloud method is apparent in Fig. 6, namely that unlike wind-tunnel methods, this method does not require a supporting rod attached to the football. The boundary-layer separation can be viewed as the football moves as it would in a typical game.

To determine the boundary-layer separation angle φ, a still image of the football passing through a dust cloud is used, along with the device is shown in Fig. 7. The device is made by cutting out a piece of cardboard a hole out whose diameter matches that of the football. The remaining cardboard is then trimmed to make an annulus about 5-cm thick, though that thickness is not important. The cardboard annulus is marked off in 5° increments, thus creating a goniometer. A blue football of the same model used in the dust-cloud tests is then inserted into the cardboard annulus so that the ball's equator fits snugly in the cardboard. The football is oriented to match the orientation of the ball in the still image of the ball passing through a dust cloud. Alligator clips and arrows cut from pink construction paper are then used to mark on the cardboard annulus the locations of the separation of the boundary layer as seen in the still images. Not only φ is determined from the cardboard goniometer, but the blue ball is viewed from the top and bottom to ascertain whether the boundary layer separated at a relatively smooth part (on one of the 32 panels) of the ball or a relatively rough part (near intersections of seams) of the ball. Taking into account the ability to determine where dust separates from the football's surface (large contributor to error) and the accuracy of the goniometer (small contributor to error), the error estimate for φ is $\pm$ 5°.

4 Results and discussion

Figure 8 shows the values of φ as the football speed is varied from 6.58 to 19.63 m/s, a range of speeds that

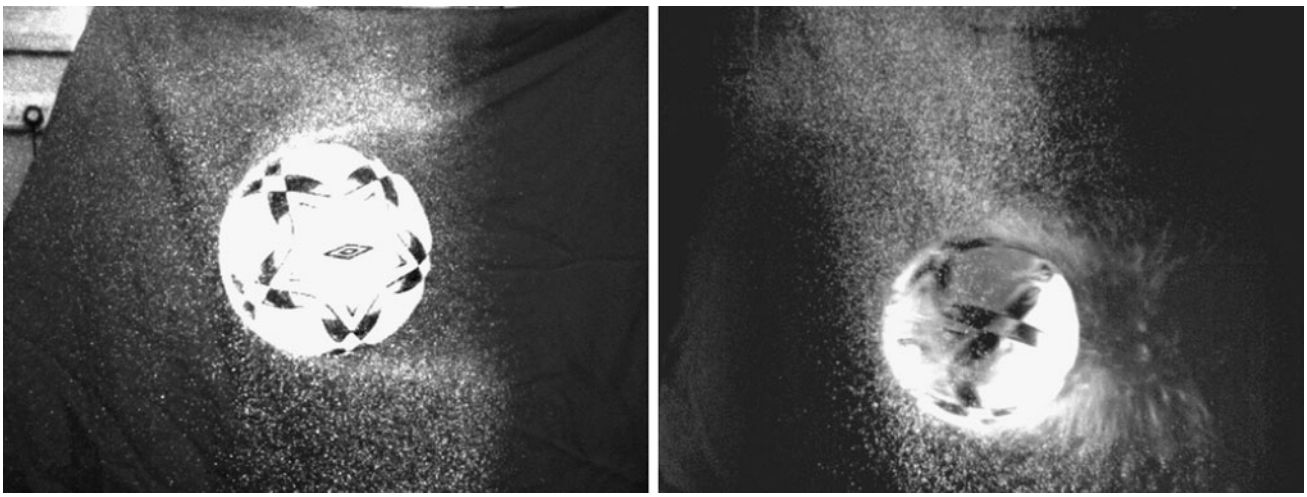

Fig. 6 Still images of a football moving at a speed below the drag crisis (*left* image) and at a speed above the drag crisis (*right* image). The ball on the left moves at 7.65 m/s and the boundary-layer separation angle is 198°. The ball on the right moves at 19.14 m/s and the boundary-layer separation angle is 97°

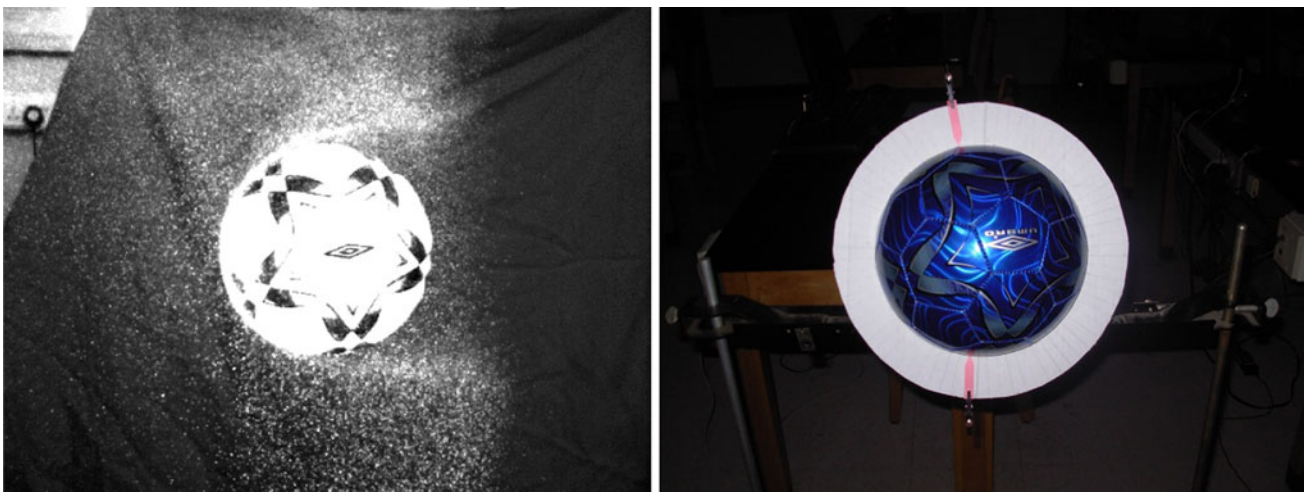

Fig. 7 A reproduction of the *left* image from Fig. 7. The cardboard annulus in the *right* image serves as a goniometer for determining φ. The markers denote where the boundary layer separates on the *top* and *bottom* of the ball

contains the drag crisis (see Fig. 2). To help put the dust tests into context, also shown in Fig. 8 is the fitted drag curve from Fig. 1. A total of 16 tests are labelled in Table 1. There are six clusters of tests to be discussed: 1–5, 6 and 7, 8 and 9, 10 and 11, 12–14, and 15 and 16.

The low-speed cluster of tests (1–5) has separation angles in the range $179° \leq \varphi \leq 206°$. A close inspection of the "Top" and "Bottom" images in Table 1 reveals that the boundary layer separated on smooth patches on the top and bottom of the ball in test 1. For tests 2–4, the boundary layer separates on a smooth patch on one side of the ball and near seams on the other side. For test 5, the boundary layer separates near seams on both the top and bottom parts of the ball. These observations are consistent with the notion that rough areas on ball surfaces delay the separation of the boundary layer [12]. Comparing test 1 with test 5, it is seen that φ drops by 27° if the boundary layer separates on the top and bottom at seams instead of at smooth patches, despite just under 2 m/s increase in centre-of-mass speed.

Tests 6 and 7 show an angular difference of 25° in φ. As expected, the boundary layer in test 6 separates at smooth patches, whereas the boundary layer in test 7 separates at seams, thus reducing φ.

As the centre-of-mass football speed is increased through the drag crisis, the boundary-layer separation behaviour becomes anomalous. Test 8 reveals a boundary-layer separation on the top and bottom to be on smooth patches, whereas test 9 reveals a boundary-layer separation at a smooth patch on the bottom and near seams at the top.

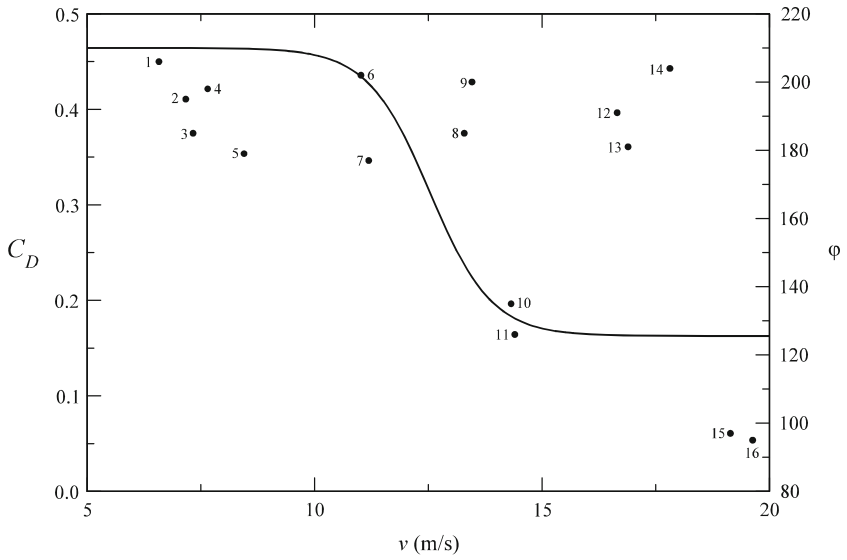

Fig. 8 The boundary-layer separation angle in degrees (*right vertical axis*) versus centre-of-mass football speed. The fitted curve for the drag coefficient (*left vertical axis*) taken from Fig. 1 is also plotted versus centre-of-mass football speed. The *numbers* next to the φ data points label the test number

Though tests 8 and 9 have their respective values of φ separated by just 15°, which is nearly close enough to be indistinguishable given the estimated error, the expected result is that the boundary layer in test 9 would have separated at a smaller angle compared to that of test 8 because of the boundary-layer separation near seams on the top part of the ball in test 9.

The boundary layer separates from the balls in tests 10 and 11 is almost exactly the same way. At the bottom of the ball, the separation is on a smooth patch; at the top of the ball, the separation is near seams. Because of the similar way in which the boundary layer separates in tests 10 and 11 and the fact that φ differs by just 9° in the two tests, it is believed that one test is an almost identical reproduction of the other test.

Of greatest interest is the cluster experiments labelled by tests 12–14. After the expected drop in φ moving from tests 8 and 9 to tests 10 and 11, an increase in φ is seen for tests 12–14 that puts that cluster of tests in a range of φ comparable to tests 1–9. Either tests 10 and 11 represent an anomalous drop in φ or tests 12–14 represent an anomalous increase in φ. Whichever the case, the authors are at present unable to explain why φ changes so rapidly for speeds in the middle of the drag crisis to speeds just past the drag crisis. It is noted that for tests 12–14, the boundary layer separates on smooth patches both at the top and bottom of the ball. That may explain why φ is larger for tests 12–14 than for tests 10 and 11, but is probably not enough to explain the size of the differential.

Tests 14 and 15 appear to be more in line with an initial understanding of boundary-layer separation. Both tests are well past the drag crisis; both tests have the boundary layer separating on a smooth patch on one side and near a junction of seams on the other side; both tests have essentially the same φ (just 2° difference). Those high-speed tests illustrate the idea that boundary-layer separation is delayed for turbulent flow compared to laminar flow.

5 Conclusions

A method has been established to examine the boundary-layer separation on sports balls, specifically footballs. The technique of using dust and a high-speed camera allows one to view the separation of the boundary layer during a football's natural flight through air. There is no need for a supporting arrangement, as is needed in wind-tunnel experiments. This technique also allows for the study of balls at speeds greater than the maximum possible test speed in some wind tunnels. Though the dust creates a bit of a mess after several trials, its use provides for a method of studying boundary-layer separation that is significantly cheaper than building/acquiring a wind tunnel.

Having established the dust method, there is a need to further examine the anomalous behaviour previously described for speeds near the drag crisis. The jump in separation angle for tests 12–14 is of great interest. A future study will include examinations in the speed range of those tests, with efforts to launch balls in such a way that the boundary layer separates on rough seams instead of smooth patches.

Another study to pursue is one that examines the boundary-layer separation on spinning footballs. The dust technique should work well for such a study. Instead of using a single still image of a non-spinning football moving through a dust cloud and then creating a single orientation of a football in the cardboard goniometer, a series of still images can be created as the ball spins through the dust cloud. The hope is to see how φ changes on a spinning ball as smooth and rough parts of the football pass near the

Table 1 Still images of dust experiments with photos of goniometer as seen from the front, top, and bottom

Test	v (m/s)	φ	Dust Image	Front	Top	Bottom
1	6.58	206°		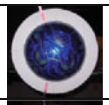	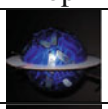	
2	7.17	195°		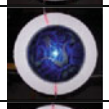		
3	7.33	185°		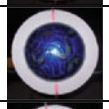		
4	7.65	198°		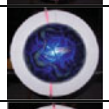		
5	8.45	179°		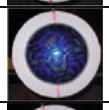		
6	11.02	202°				
7	11.19	177°		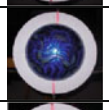		
8	13.29	185°		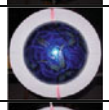		
9	13.46	200°		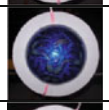		
10	14.32	135°		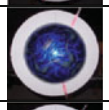		
11	14.40	126°				
12	16.65	191°				
13	16.89	181°				
14	17.81	204°				
15	19.14	97°				
16	19.63	95°				

The top and bottom images allow one to determine the nature of the ball's surface where the boundary layer separates

boundary-layer separation points. For each still frame of a spinning ball moving through a dust cloud, one can recreate the configuration with the goniometer.

Acknowledgments The authors thank University of Sheffield sports engineering postgraduate students Sarah Tomlinson, Nick Emerson, and James Clarke for their assistance with the dust experiments.

References

1. Achenbach E (1974) The effects of surface roughness and tunnel blockage on the flow past spheres. J Fluid Mech 65:113–125. doi:10.1017/S0022112074001285
2. Carré MJ, Goodwill SR, Haake SJ (2005) Understanding the effect of seams on the aerodynamics of an association football. Proc IMechE Part C: J Mech Eng Sci 219:657–666. doi:10.1243/095440605X31463
3. Asai T, Seo K, Kobayashi O, Sakashita R (2007) Fundamental aerodynamics of the soccer ball. Sports Eng 10:101–110. doi:10.1007/BF02844207
4. Alam F, Chowdury H, Moria H, Fuss FK (2010) A comparative study of football aerodynamics. Procedia Eng 2:2443–2448. doi:10.1016/j.proeng.2010.04.013
5. Oggiano L, Soetran L (2010) Aerodynamics of modern soccer balls. Procedia Eng 2:2473–2479. doi:10.1016/j.proeng.2010.04.018
6. Barber S, Chin SB, Carré MJ (2009) Sports ball aerodynamics: a numerical study of the erratic motion of soccer balls. Compt Fluids 38:1091–1100. doi:10.1016/j.compfluid.2008.11.001
7. Goff JE, Carré MJ (2009) Trajectory analysis of a soccer ball. Am J Phys 77:1020–1027. doi:10.1119/1.3197187
8. Goff JE, Carré MJ (2010) Soccer ball lift coefficients via trajectory analysis. Eur J Phys 31:775–784. doi:10.1088/0143-0807/31/4/007
9. Choppin S, Kelley J (2010) Generating football Cd profiles without a wind tunnel. Procedia Eng 2:2449–2454. doi:10.1016/j.proeng.2010.04.014
10. Barber S, Carré MJ (2010) The effect of surface geometry on soccer ball trajectories. Sports Eng 13:47–55. doi:10.1007/s12283-010-0048-x
11. Hong S, Chung C, Nakayama M, Asai T (2010) Unsteady aerodynamic force on a knuckleball in soccer. Procedia Eng 2:2461–2466. doi:10.1016/j.proeng.2010.04.015
12. Mehta RD (1985) Aerodynamics of sports balls. Ann Rev Fluid Mech 17:151–189. doi:10.1146/annurev.fl.17.010185.001055